ASM Sc. J., 19, 2024

https://doi.org/10.32802/asmscj.2023.1758

Switchable Dual-Wavelength Q-Switched Erbium-Doped Fibre Laser using Spider Silk as a Biocompatible and Eco-Friendly Saturable Absorber

N.A.M. Muhammad[1], N.A. Awang[1*] and M.I. Supaat[2]

[1]*Photonics Devices Sensors Research (PDSR), Faculty of Applied Sciences and Technology, Universiti Tun Hussein Onn Malaysia, Pagoh Higher Education Hub, KM1 Jalan Panchor, 84600 Panchor, Johor, Malaysia*

[2]*SIGTECH Engineering Sdn. Bhd., No. 12A, Jalan Dagang SB 4/1, Taman Sungai Besi Indah Selangor, Seri Kembangan, 43300, Selangor, Malaysia*

This work aims to study the dual-wavelength Q-switched fibre laser performances with erbium-doped fibre as the gain medium and the fibre Bragg gratings to allow stable switchable dual-wavelength states. Spider silk was used as an alternative biological material for saturable absorber. The spider silk as a saturable absorber was prepared by directly sandwiched between the surface of fibre ferrules. A dual-wavelength system operating at 1550 nm and 1560 nm was generated by modulating the polarisation controller to regulate the mode competition in the ring cavity. This allows for a flexible switch between individual wavelengths of 1550 nm or 1560 nm. The device operates at a wavelength of 1550 nm, with 26.63 kHz repetition rate and 9.45 µs pulse width. At a wavelength of 1560 nm, it produces a repetition rate of 24 kHz and a pulse width of 10.47 µs. The output demonstrated consistent stability throughout time, with no changes recorded. This indicates a stable signal-to-noise ratio of 41.12 dB and 34 dB for wavelengths 1550 nm and 1560 nm, respectively. This study presents the latest approach using spider silk as a saturable absorber to create a dual-wavelength Q-switched fibre laser. The laser is based on a fibre Bragg gratings device and has potential uses in terahertz signal and laser radar.

Keywords: biocompatible; biological material; dual-wavelength; eco-friendly; erbium-doped fibre laser; fibre Bragg gratings; fibre optic; passively Q-switched; saturable absorber; spider silk

*Corresponding author's e-mail: norazura@uthm.edu.my

I. INTRODUCTION

Dual-wavelength Q-switched fibre laser is a highly adaptable light source that can emit more than a single discrete laser emission line. While, switchable dual-wavelength fibre laser implies the ability to adjust the laser emission rapidly and discretely from one fixed wavelength to another predefined wavelength, which has drawn significant attention in various fields of applications, including biomedical research (Al-Karadaghi *et al.*, 2015), fibre optic sensing (Du *et al.*, 2019; Yin *et al.*, 2019; Arman & Olyaee, 2021; Sardar *et al.*, 2021), millimetre wave (Yu *et al.*, 2006), optical communication systems, microwave photonics (Yao *et al.*, 2006; Pan & Yao, 2009b; Pan & Yao, 2009a; Jiang *et al.*, 2011; Wang *et al.*, 2015), remote sensing instruments (Sharma *et al.*, 2004; Han *et al.*, 2005), spectroscopy (Krzempek *et al.*, 2013) and terahertz signal (Gu *et al.*, 1998; Kleine-Ostmann & Nagatsuma, 2011; Tang *et al.*, 2011; Soltanian *et al.*, 2015). Dual-wavelength Q-switched fibre laser consists of a basic Q-switched configuration component, two selective wavelength elements of the fibre Bragg grating device, and a polarisation controller, which is necessary to obtain switchable dual-wavelength operation and to reflect at different wavelengths. Fibre Bragg grating operates as a wavelength-selective element, which is carefully structured with distinct grating periods that align with the targeted wavelengths at which they reflect light (Erdogan, 1997; Lin *et al.*, 2001). The fibre Bragg grating's design parameters, such as the period and amplitude of the refractive index modulation, determine the specific wavelength that the grating reflects. When light travels through an optical fibre, the fibre Bragg grating causes the reflection of the Bragg wavelength, leading to a distinct reflection peak at that specific wavelength, and at the same time transmits all others.

A saturable absorber is essential to passively Q-switched, which is an optical device or material that exhibits a nonlinear response to incident light. It is featured by the potential to modulate the light intensity passing through them, depending on the intensity of the incident light. The mechanism of a saturable absorber is based on the concept of intensity-dependent transmission or absorption of light (Kashiwagi *et al.*, 2010). It is classified either as an artificial or real saturable absorber. Artificial saturable absorbers such as nonlinear polarisation rotation (Durán-Sánchez *et al.*, 2023), non-linear optical loop mirrors (Ibarra-Escamilla *et al.*, 2018), and nonlinear optical amplified mirrors (Duran-Sanchez *et al.*, 2022) have the advantages of ultrafast response. However, they can easily be influenced by environmental conditions, which limits their application. On the other hand, real saturable absorbers are one of the most widely used techniques to produce dual-wavelength Q-switched fibre laser, they have higher environmental persistence than artificial saturable absorbers. Additionally, they can be simply incorporated into an optical fibre (Ainnaa Mardhiah Muhammad *et al.*, 2023). Common real saturable absorbers are used, which include calcium carbonate nanoparticles, graphene, molybdenum sulfoselenide, topological insulator, tungsten sulfide, and zinc oxide-titanium dioxide nanoparticles (Guo *et al.*, 2015; Li *et al.*, 2019; Yusoff *et al.*, 2019; Ali *et al.*, 2021; Muhammad *et al.*, 2022; Jasem *et al.*, 2023; Muhammad *et al.*, 2023). Despite the existence of a variety of saturable absorbers, there has been a lack of emphasis on valuable biological saturable absorbers, such as spider silk. Natural spider silk is a type of protein-based biological material produced by spider naturally through the silk gland in the bodies (Kiseleva *et al.*, 2020). In response to the growing need for sustainable development, natural spider silk became an ideal alternative for use as a saturable absorber in the formation of dual-wavelength Q-switched pulse fibre laser as it can produce the pulse at a very short time due to fast recovery, which means that they can quickly return to their transparent or low absorption state after absorbing a high-intensity laser pulse. The fast recovery time possessed by spider silk is due to the transparency of spider silk corresponding to the optical transparency of the fibre. It enables efficient transmission of light, by minimising the losses of the cavity created thus facilitating the creation of intense laser pulses. Previous studies have demonstrated that spider silk possesses unique properties that allow it to transmit light. This capability is attributed to the specific protein structure inherent in spider silk (Huby *et al.*, 2013a; E *et al.*, 2022; Li *et al.*, 2022). The tensile strength of spider silk that may surpass some max phases material is believed to

maintain the stability of the pulse will be generated within the laser system ensuring consistent performance during the Q-switching operation. Furthermore, it can be utilised as an effective saturable absorber in fibre laser structures without the need for complex procedures or particular components. Inherently more versatile and can adapt to various environmental conditions, which may not be the case for alkali metals as spider silk has been shown to maintain its functionality and longevity over an extended period due to high resistance to optical damage and degradation under different operating conditions (Huby *et al.*, 2013a; Qiao *et al.*, 2017; Hey Tow *et al.*, 2018; E *et al.*, 2022; Muhammad *et al.*, 2024). We used a biological material of spider silk as a saturable absorber material instead of organic material, max phases, and alkali metal due to spider silk is a biocompatible and sustainable material that coincides with the increasing need for eco-friendly and bio-inspired technologies. The environmental footprint of laser technology can be neutralised by selecting spider silk as a saturable absorber. This could have implications for applications in biomedicine, bio-optical sensing, and biochemical fields, all of which require biocompatibility (Vehoff *et al.*, 2007; Fu *et al.*, 2009; Huby *et al.*, 2013b; Hey Tow *et al.*, 2018; E *et al.*, 2022; Li *et al.*, 2022).

In this study, a straightforward method of dual-wavelength Q-switched erbium-doped fibre laser was experimentally generated from a biological material of spider silk as a saturable absorber, together with the utilisation of fibre Bragg gratings. Here, spider silk was sandwiched between the surfaces of fibre ferrules. In our laser configuration, we have successfully demonstrated the ability to switch between two different wavelengths. This was accomplished by using two fibre Bragg gratings as a coarse wavelength selector. Additionally, we used a spider silk-based saturable absorber to realise Q-switched operation. As a result, a stable dual-wavelength Q-switched pulse fibre laser was attained with central wavelengths of 1550 nm and 1560 nm. In addition, precise manipulation of the polarisation controller allows for the attainment of dominant-wavelength Q-switched operation at either 1550 nm or 1560 nm. This enables the convenient switching between the two wavelengths as desired. As far as we know, this is the first instance where spider silk is being used as a saturable absorber to successfully create a dual-wavelength Q-switched pulse erbium-doped fibre laser experiment.

II. EXPERIMENTAL

The spider silk sample was prepared using the same technique as described in (Muhammad *et al.*, 2024), specifically in Section 2.1 and Section 2.2. Figure 1 displays the configuration of the proposed switchable dual-wavelength Q-switched erbium-doped fibre laser with a gain medium that was selected consisting of highly erbium-doped fibre, specifically the I-12(980/125)HC with a length of 3 meters. All of the other fibres used were classed as standard single-mode fibres. The erbium-doped fibre was excited by a laser diode operating at a wavelength of 980 nm, which was spliced to a 980/1550 nm wavelength division multiplexer. A configuration using the concatenation of two fibre Bragg gratings was deployed as a coarse wavelength selector, with defined central wavelengths of 1550 nm and 1560 nm, respectively. The polarisation controller was used in between the two fibre Bragg gratings to set the intracavity birefringence (to split the optical signal). The unidirectional performance of the fibre laser was ensured through the use of a circulator, which was positioned between erbium-doped fibre and a 90:10 optical coupler. A 10 % port of optical coupler was tapped out from the ring cavity, to obtain the output signal, while the remaining 90 % serves as feedback within the cavity. Between the 90:10 optical coupler and the optical isolator, the silk directly collected from the jumping spider of *Plexippus sp*. was introduced as a saturable absorber. The optical spectrum analyser (OSA; Yokogawa, AQ6370D) was used to monitor and evaluate the signal analysis within the optical spectrum. The measurement of the pulse train and frequency domain was conducted using the Tektronix MDO3104 oscilloscope in conjunction with the 5 GHz InGaAs biased detector (Thorlabs, DET08CFC/M) photodetector.

In dual-wavelength Q-switched, the fibre laser cavity is designed to support two distinct wavelengths simultaneously. The Q-switched mechanism involves controlling the quality factor (Q factor) of the laser cavity, which regulates the pulse generation. The polarisation controller manipulates the polarisation state of light, impacting the Q-switched operation. Fibre Bragg gratings, acting as wavelength-selective mirrors, assist in generating dual-wavelength pulses. Spider silk saturable absorber modulates the laser intensity, contributing to the Q-switched. A detailed explanation, the generation of Q-switched pulses takes place by initiating a photon of light that will enter the core of the erbium-doped fibre. This erbium-doped fibre serves as the gain medium in the laser cavity to amplify light. Erbium ions contained in this fibre will help to absorb the energy supply from the pump diode. The energy will be transferred to erbium ions creating a population inversion meaning that the exceed ion is at a higher state rather than ground state ions. The pump diode will continuously supply energy to gain medium, thus maintaining the creation of population inversion. Following that, the light will continue to enter spider silk saturable absorber material. In fact, saturable absorber material is designed to have high absorption material, creating high losses within the laser cavity thus inhibiting lasing from occurrence. As mentioned before, the pump diode continuously supplies energy to gain medium. After a specific time, the energy contained within the gain medium achieved a threshold value that is higher than the loss of cavity created by the spider silk saturable absorber, causing the absorption of the spider silk saturable absorber to suddenly become saturated and then move to a transparent state. At this moment, the loss of the cavity will be reduced and the accumulation of energy contained in the gain medium will be released thus forming the Q-switched pulse with high energy and short intensity. After the pulse was generated, the spider silk saturable absorber seemed to bring themselves to the recovery phase, preparing for the next round of lasing. During this time, the spider silk saturable absorber returns to its high absorption state, causing high losses of the cavity and inhibited lasing. The pump diode continues to supply energy to gain medium, readying themselves for the next cycle. The entire process repeats itself. As the spider silk saturable absorber recovers, the loss in the cavity increases, inhibiting lasing. The energy of the gain medium continues to be accumulated once again until reaching the threshold value, and the spider silk saturable absorber switches state, leading to the generation of the Q-switched pulses.

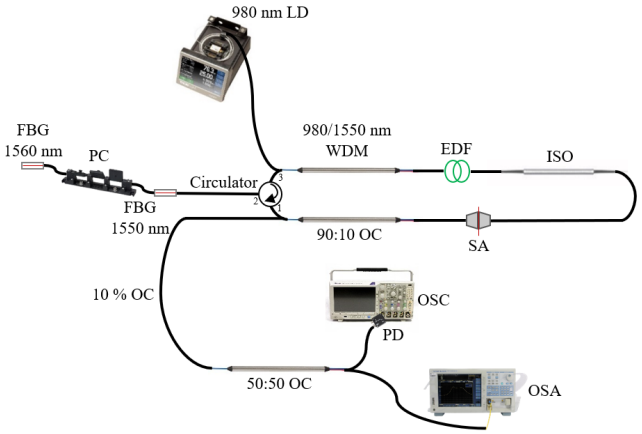

Figure 1. Schematic configuration of switchable dual-wavelength Q-switched erbium-doped fibre laser with spider silk as a saturable absorber.

III. RESULT AND DISCUSSION

A. Characterisation

Our study previously conducted, revealed the detailed characteristics of spider silk to act as a saturable absorber according to reference (Muhammad *et al.*, 2024).

B. Switchable Dual-wavelength Q-switched erbium-doped Fibre Laser

In this experimental configuration, the occurrence of continuous-wave lasing was noticed when the pump power reached a threshold value of 34 mW. Furthermore, the self-starting Q-switched pulse was generated once the input pump power reached 41 mW. The steady pulse patterns were seen until the pump power reached a value of 151.40 mW. When the pump power exceeds 151.40 mW, the pulse train becomes unstable. However, reducing the input power value below 151.40 mW results in the recurrence of steady pulses. This observation suggests that the structural integrity of the saturable absorber was not compromised. The presence of an unstable pulse train, which absorbed below 47.20 mW value, can be attributed to the insufficient pump power required for the lasing action of a dual-wavelength Q-switched fibre laser.

The polarisation controller was adjusted, and dual-wavelength Q-switched output was formed as a result of these adjustments. Figure 2 shows the presence of the output spectrum dual-wavelength, λ_c at 1550 nm and 1560 nm with the distance between the peaks, $\Delta\lambda$ of dual-wavelength by 1 nm. The corresponding output power, P values were -24.73 dBm and -25.31 dBm, respectively. The dual-wavelength Q-switched pulse train, exhibiting a repetition rate of 25.67 kHz, was achievable as in Figure 3. The pulse width and peak intensity of this pulse train were identified to be 9.45 µs and 0.20 arb. unit, respectively. Additionally, there are two asynchronous pulse trains (harmonic frequency), which indicates the repetition rates of the two wavelengths are slightly different. According to the data presented in Figure 4, the related radio frequency spectrum was also quantified, utilising a resolution bandwidth of 600 Hz, confirming that the two asynchronous pulse trains of the dual-wavelength pulses have two peaks operate around the fundamental repetition rate of 25.67 kHz and the radio frequency spectrum under the 1st and 2nd orders harmonic has a repetition rate of 25 kHz and 38 kHz, respectively. The calculated signal-to-noise ratio value was nearly 39 ± 11 dB, suggesting stability of the pulse system.

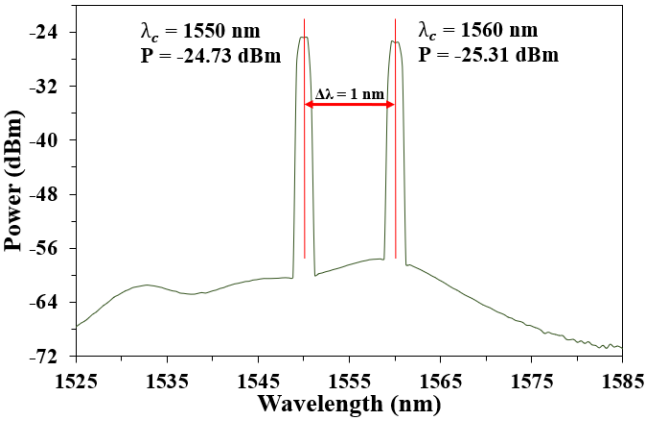

Figure 2. Output optical spectrum for dual-wavelength Q-switched pulse erbium-doped fibre laser at pump power value of 151.40 mW.

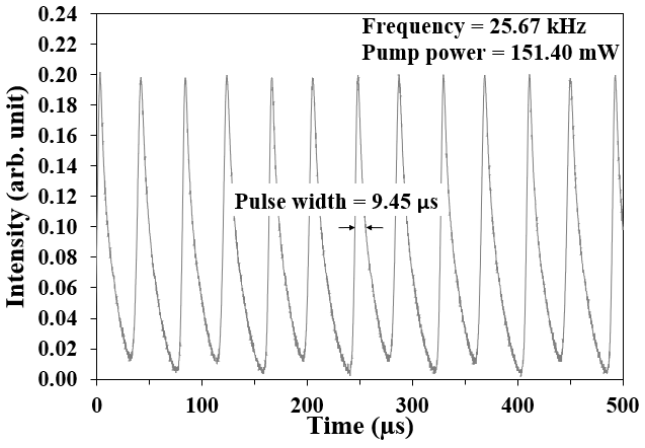

Figure 3. Oscilloscope trace of dual-wavelength Q-switched pulses.

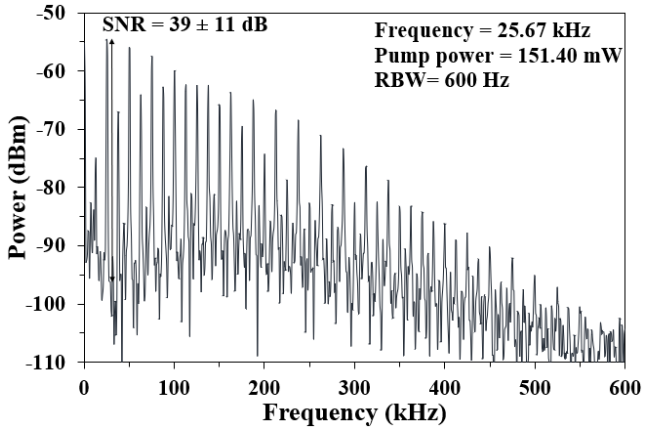

Figure 4. The radio frequency spectrum of dual-wavelength Q-switched pulses.

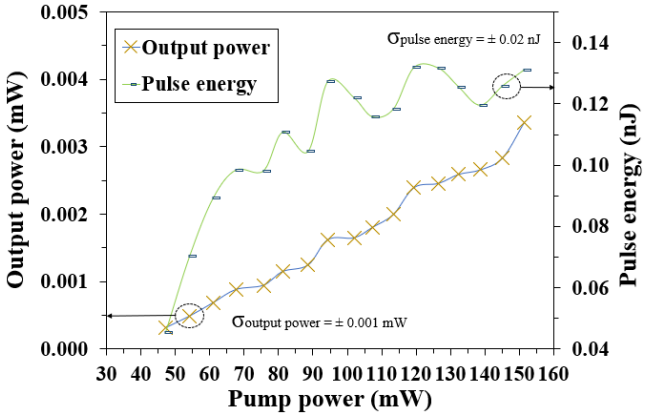

Figure 5. Graph depicting the relationship between output power and pulse energy as a function of pump power.

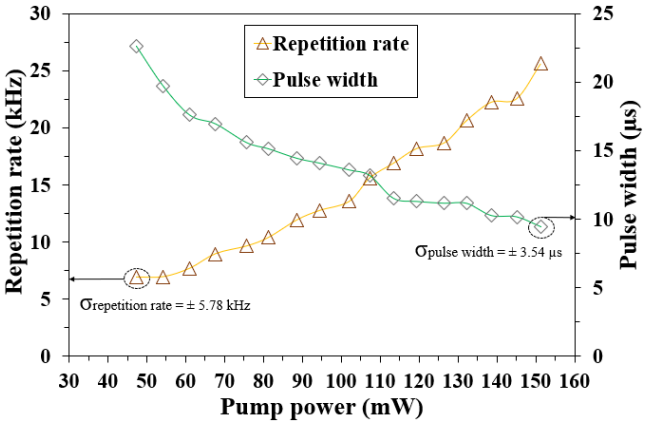

Figure 6. Graph portraying the relationship between repetition rate and pulse width versus pump power.

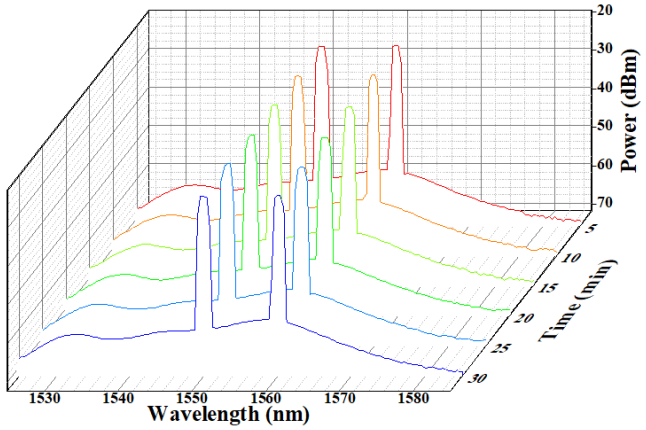

Figure 7. The long-term stability of dual-wavelength Q-switched erbium-doped fibre laser.

Figure 5 and Figure 6 emphasise the progression of the dual-wavelength Q-switched pulse characteristics through the pump power was incrementally increased from 47.20 mW to 151.40 mW while maintaining a polarisation controller condition. As indicated in Figure 5, there was a noticeable increase in both the output power and the pulse energy as the pump power was varied. Specifically, the output power ranges from 0.0003 mW to 0.003 ± 0.001 mW, while the pulse energy ranges from 0.05 nJ to 0.13 ± 0.02 nJ. Once the pump power goes over 151.40 mW, the operation of the Q-switched becomes unstable. Continued augmentation of the pump power will lead to a transition from Q-switched to continuous-wave operation; however, this state can be restored by subsequently reducing the pump power. The graphical representation in Figure 6 clarifies the relationship between the repetition rate and pulse width as they evolve with varying pump power levels. When the repetition rate of the Q-switched pulses was increased from 6.92 kHz to 25.67 ± 5.78 kHz, there was a continuous decrease in the pulse width from 22.65 μs to 9.45 ± 3.54 μs. The long-term stability of the dual-wavelength Q-switched pulse is displayed in Figure 7. Data was collected every five minutes during half of an hour observation of a stable dual-wavelength Q-switched pulse fibre laser. Over this duration, there was no attenuation of amplitude or change in pulse form.

The switchable dual-wavelength pulse fibre laser by controlling the polarisation controller was further demonstrated. Likewise, at a pump power value of 151.40 mW, the recorded output optical spectrum, pulse train, and

radio frequency spectrum at the corresponding wavelengths of 1550 nm and 1560 nm are illustrated below.

Figure 8 displays a peak wavelength of 1550 nm, accompanied by an output power of -23.07 dBm. In Figure 9, the pulse train is depicted, with the 26.63 kHz repetition rate corresponding to a pulse width of 9.45 µs, as calculated from the full width at half maximum of a single pulse with the intensity of this pulse was roughly 0.19 arb. unit. The radio frequency spectrum representation of the output pulse train is shown in Figure 10. The spectrum analysis verifies that the fundamental harmonic exhibits a frequency of 26.63 kHz, with the signal-to-noise ratio of 41.12 ± 10.02 dB was determined by comparing the high power and low power levels within the frequency spectrum. The characteristics of switchable dual-wavelength Q-switched fibre lasers were further interpreted. Specifically, the focus is on analysing the pulse repetition rate, pulse width, output power, and pulse energy in relation to the pump power. The pump power was increased from 47.20 mW to 151.40 mW, with all other variables remaining constant. In Figure 11, the relation of pulse repetition rate and pulse width can be seen as a function of the pump power. The observed data indicates an increase in the pulse repetition rate from 8.04 kHz to 26.63 ± 5.85 kHz, accompanied by a notable decrease in pulse width from 18.95 µs to 9.45 ± 2.60 µs. Additionally, the output power and the accompanying computed pulse energy were obtained, as illustrated in Figure 12. The increase in the pump power results in increases in both the output power from 0.0005 mW to 0.005 ± 0.001 mW and pulse energy from 0.07 nJ to 0.19 ± 0.04 nJ.

However, the pulse energy curve in Figure 5 and Figure 12 fluctuates and does not increase linearly due to the dynamics interplay between the gain, losses, and Q-switched mechanisms. The inherent nonlinear process to generate a Q-switched pulse includes the accumulation of energy in the gain medium, followed by the sudden release of energy being stored, and then the formation of the pulses, which lead to variations in pulse energy. Furthermore, the dual-wavelength fibre laser operation brings additional complexities, which means the interaction between different wavelengths leads to mode competition and fluctuates in the energy level of each wavelength. Next, the sensitivity of the fibre laser system to external conditions, such as temperature fluctuations or mechanical vibrations, can also contribute to nonlinear behaviour. These external factors introduce instabilities in the laser cavity, affecting the pulse generation process.

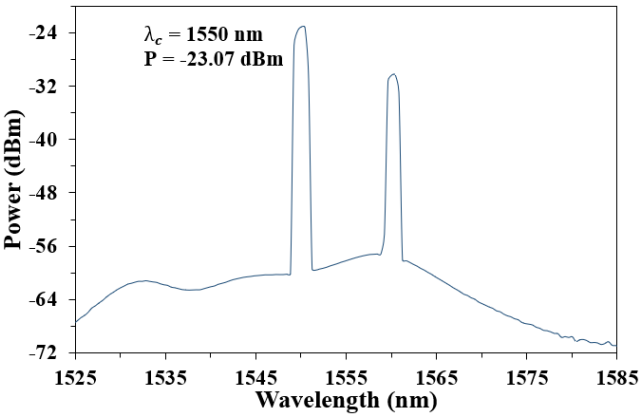

Figure 8. The output optical spectrum at 1550 nm dominant dual-wavelength.

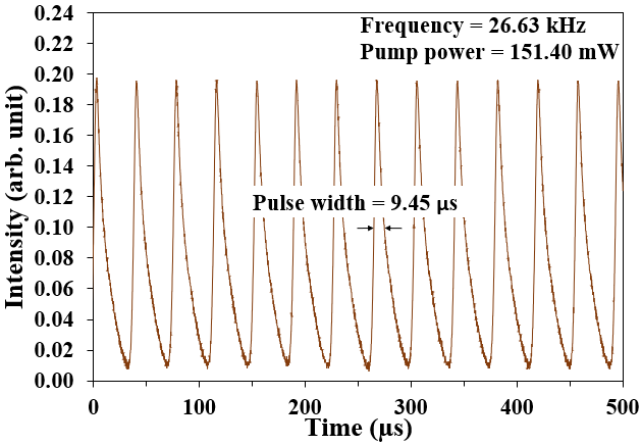

Figure 9. The pulse train at 1550 nm dominant dual-wavelength.

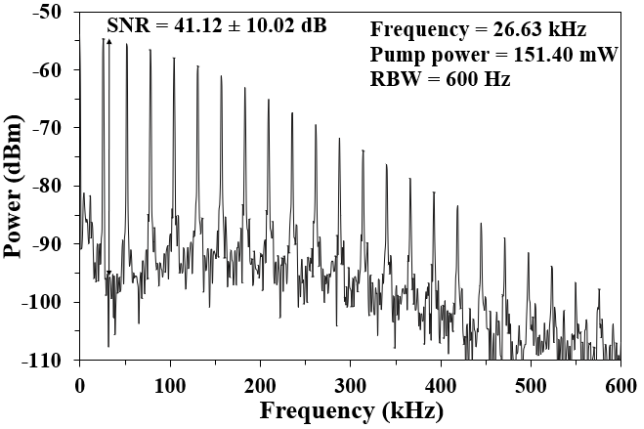

Figure 10. The radio frequency spectrum at 1550 nm dominant dual-wavelength.

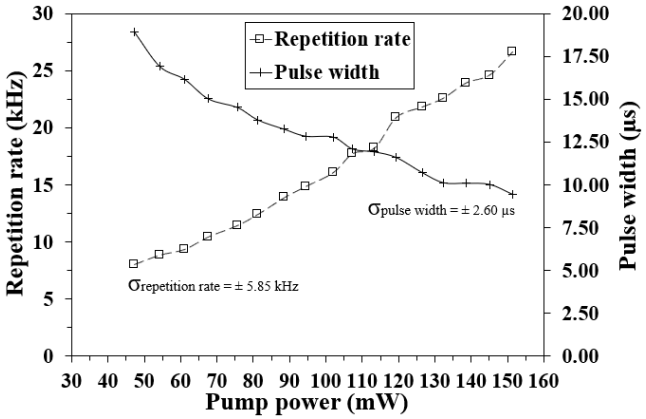

Figure 11. The correlation between repetition rate and pulse width as a function of pump power.

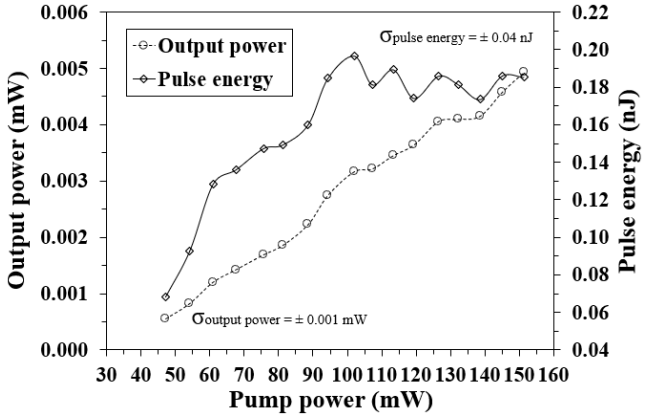

Figure 12. The correlation of output power and pulse energy against pump power.

In the meantime, Figure 13 exhibits the dominant wavelength at the peak of the 1560 nm spectrum, featuring an output power of -23.10 dBm. In Figure 14, the pulse train was seen, with a repetition rate of 24 kHz and a pulse width of 10.47 µs, as calculated from the full width at half maximum of an individual pulse. The wavelength of 1560 nm likewise has a stable signal-to-noise ratio of 34 ± 12 dB measured from the radio frequency spectrum of the pulses under harmonic characteristics possessing the repetition rate of 24 kHz and 36 kHz, respectively, as indicated in Figure 15. Figure 16 presents a trend of the characteristic features commonly observed in Q-switched pulse fibre laser. It demonstrates a notable increase in the pulse repetition rate, ranging from 6.45 kHz to 24 ± 5 kHz. This increase was accompanied by a matching decrease in pulse width, which reduced from 24 µs to 10.47 ± 3.30 µs. In addition to this, the output power and the related predicted pulse energy were measured, as in Figure 17. The values of output power and pulse energy were determined at 0.0006 mW to 0.005 ± 0.001 mW and 0.10 nJ to 0.20 ± 0.03 nJ exhibiting a linear relationship with the pump power, increased from 47.20 mW to 151.40 mW.

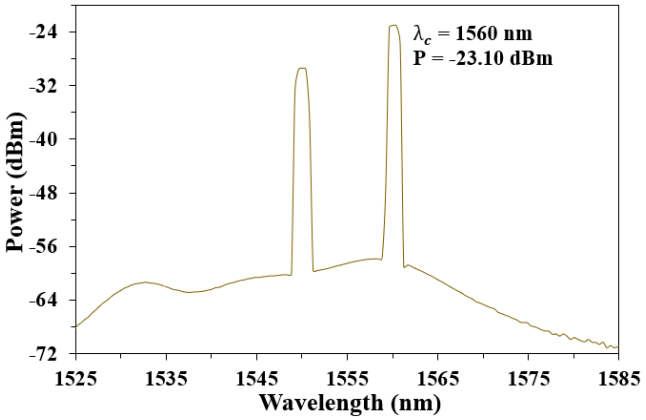

Figure 13. The output spectrum at 1560 nm dominant dual-wavelength.

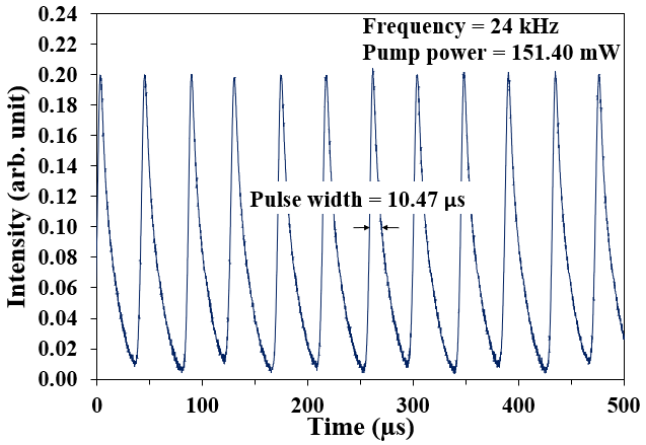

Figure 14. The pulse train at 1560 nm dominant dual-wavelength.

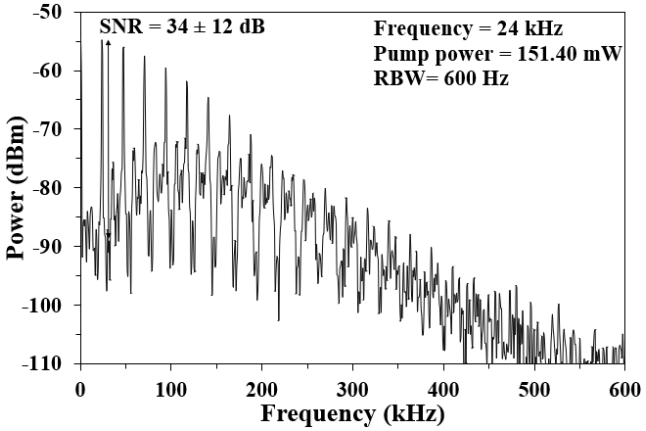

Figure 15. The radio frequency spectrum at 1560 nm dominant dual-wavelength.

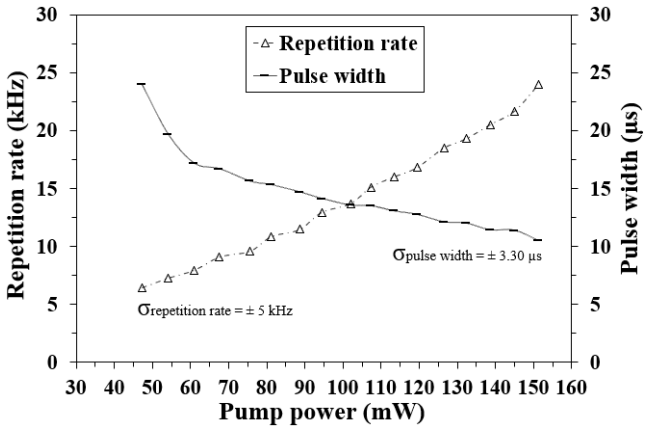

Figure 16. Relationship between repetition rate and pulse width against pump power.

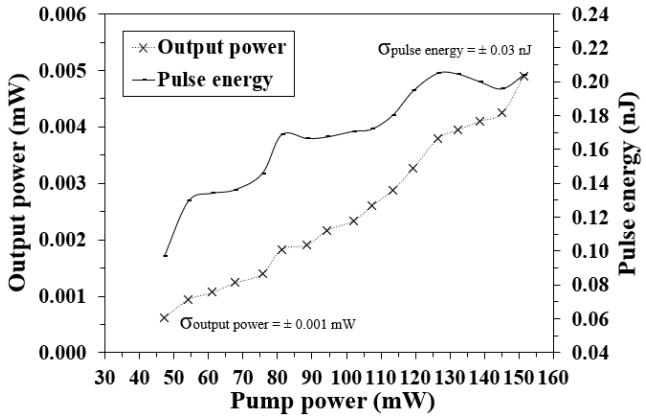

Figure 17. Relationship between output power and pulse energy against pump power.

Both figures reveal the phenomenon of mode competition in erbium-doped fibre, which arises from the combined effects of cross-gain saturation and substantial homogeneous line broadening. These factors significantly impact the active gain medium and contribute to the observed competition between two wavelengths (Ahmad *et al.*, 2019). The dual-wavelength output tends to lase at only the dominant wavelength due to the polarisation hole-burning effect of erbium-doped fibre (Zhang *et al.*, 2012). In this situation, the utilisation of a polarisation controller for the manipulation of light's polarisation state and the prevention of homogeneous broadening can bring in a transition to the prevailing wavelength, where the fibre Bragg gratings serve as the selector for the specific wavelength.

To analyse the performance of the dual-wavelength Q-switched in comparison with other saturable absorbers, the output characteristics based on different saturable absorbers are listed in Table 1. As shown in the table, the obtained results in this work are comparable with other saturable absorbers reported in the literature in terms of pulse width, repetition rate, signal-to-noise ratio (SNR), and input pump power. In 2013, Liu *et al.* (2013) presented and demonstrated the creation of a dual-wavelength Q-switched erbium-doped fibre laser based on a single-wall carbon nanotube saturable absorber. Chen *et al.* (2020) in 2020 conducted an experimental study where they successfully developed a single or dual-wavelength switchable and tunable passively Q-switched erbium-doped fibre laser based on a semiconductor saturable absorber mirror (SESAM). The experimental setup utilises a birefringent Sagnac loop mirror that combines the gain spectrum enabling the laser to operate in tunable and switchable single or dual-wavelength states. The system exhibits a simultaneous oscillation at two different wavelengths, particularly 1556.84 nm and 1562.11 nm, with a separation of 5.27 nm between the two wavelengths. In the same year, Zalkepali *et al.* (2020) employed a pulsed fibre laser with an indium-tin oxide as a saturable absorber on a fibre ferrule which was fabricated via direct current magnetron sputtering. The purpose was to produce a dual-wavelength erbium-doped fibre laser at peaks of 1532 and 1533 nm, which could be switched on and off. Subsequently, Najm *et al.* (2023) generated a stable dual-wavelength output using a molybdenum titanium aluminium carbide. The laser operated at wavelengths of 1531.6 nm and 1557 nm and achieved a signal-to-noise ratio of 70 dB.

Table 1. Comparison performances of dual-wavelength Q-switched with previous works.

Saturable absorber material	Fabrication	Min. pulse width (μs)	Max. repetition rate (kHz)	SNR (dB)	Wavelength (nm)		Input pump power (mW)	Ref.
					Short region	Long region		
Single-wall carbon nanotube	Chemical vapour deposition	2.6 (1532 nm) 3.3 (1558 nm)	66.2	-	1532	1558	108	(Liu *et al.*, 2013)
SESAM	-	2.91	58.57	49	1556.84	1562.11	300	(Chen *et al.*, 2020)
Indium tin oxide	DC magnetron sputtering	6.8	36.3	65.68	1532	1533	118.10	(Zalkepali *et al.*, 2020)
Molybdenum titanium aluminium carbide	Mechanical exfoliation	2.7	126	70	1531.6	1557	167	(Najm *et al.*, 2023)
Spider silk	Mechanical exfoliation	9.45	25.67	39	1550	1560	151.40	This work

IV. CONCLUSION

In this work, spider silk as a saturable absorber was successfully sandwiched between the surfaces of the fibre ferrules as well as fibre Bragg gratings were inserted in a ring cavity to help generate a dual-wavelength Q-switched fibre laser. The laser has the capability to function in dual and switched to dominant wavelength Q-switched fibre laser modes, which can be easily switched by precisely adjusting the polarisation controller. A dual-wavelength Q-switched fibre laser operating at 1550 nm and 1560 nm have been successfully developed. The laser achieves a repetition rate of 26.63 kHz and 24 kHz, with the pulse width of 9.45 μs and 10.47 μs, respectively. These output parameters were obtained at a pump power of 151.40 mW. Furthermore, it is noted that the output signal exhibits no variation over time, demonstrating stability with a signal-to-noise ratio of 41.12 dB and 34 dB at wavelengths 1550 nm and 1560 nm, correspondingly. Our findings indicate that the combination of a spider silk saturable absorber and fibre Bragg gratings shows promise as a suitable option for a dual-wavelength Q-switched fibre laser.

V. ACKNOWLEDGEMENT

This research was supported by Universiti Tun Hussein Onn Malaysia (UTHM) through Research Enhancement Graduate Grant (RE-GG) (UTHM/PS/500-19/7/4) (grant number, Q058).

VI. REFERENCES

Ahmad, H, Zainudin, FM, Azmi, AN, Thambiratnam, K, Ismail, MF, Aminah, NS & Zulkifli, MZ 2019, 'Compact L-band switchable dual wavelength SOA based on linear cavity fiber laser', *Optik*, vol. 182(January), pp. 37–41. doi: 10.1016/j.ijleo.2019.01.003.

Ainnaa Mardhiah Muhammad, N, Azura Awang, N, Noor Haryatul Eleena Nik Mahmud, N, Ummi Hazirah Hani Zalkepali, N, Zamira Muhamad Zamri, A, Basri, H & Izwanie Rasli, N 2023, 'Biosynthesized zinc oxide and titanium dioxide nanoparticles by aloe vera extract for tunable Q-switched application', *Optical Fiber Technology*, vol. 77(February), p. 103276. doi: 10.1016/j.yofte.2023.103276.

Ali, UUM, Harun, SW, Zulkipli, NF, Rosol, AHA, Rahman, HA, Jusoh, Z & Yasin, M 2024, 'Simultaneous dual-wavelength q-switched fiber laser utilizing tungsten sulfide as saturable absorber', *Chalcogenide Letters*, vol. 18, no. 10, pp. 601–606.

Al-Karadaghi, TS, Gutknecht, N, Jawad, HA, Vanweersch, L & Franzen, R 2015, 'Evaluation of Temperature Elevation During Root Canal Treatment with Dual Wavelength Laser: 2780 nm Er, Cr:YSGG and 940 nm Diode', *Photomedicine and Laser Surgery*, vol. 33, no. 9, pp. 460–466. doi: 10.1089/pho.2015.3907.

Arman, H & Olyaee, S 2024, 'Realization of low confinement loss acetylene gas sensor by using hollow-core photonic bandgap fiber', *Optical and Quantum Electronics*, vol. 53, no. 6, pp. 1–13, viewed 27 December 2023, <https://link.springer.com/article/10.1007/s11082-021-02969-x>.

Chen, S, Lu, B, Wen, Z, Chen, H & Bai, J 2020, 'Single/dual-wavelength switchable and tunable passively Q-switched erbium-doped fiber laser', *Infrared Physics and Technology*, vol. 111(July), p. 103519. doi: 10.1016/j.infrared.2020.103519.

Du, X, Liu, X, Zhang, X & Yang, J 2019, 'Dual-ring dual-wavelength fiber laser sensor for simultaneous measurement of refractive index and ambient temperature with improved discrimination and detection limit', *Applied Optics,* vol. 58, no. 27, pp. 7582–7587, viewed 27 December 2023, <https://opg.optica.org/viewmedia.cfm?uri=ao-58-27-7582&seq=0&html=true>.

Duran-Sanchez, M *et al.* 2022, 'Dark Rectangular Pulses From a Dumbbell-Shaped Mode-Locked Double-Clad Er:Yb Laser', *IEEE Photonics Technology Letters*, vol. 34, no. 21, pp. 1147–1150. doi: 10.1109/LPT.2022.3203666.

Durán-Sánchez, M *et al.* 2023, 'Passively Q-switched mode-locked thulium-doped fiber laser using nonlinear polarization rotation technique', *Ceramics International*, vol. 49, no. 24, pp. 41230–41237. doi: 10.1016/j.ceramint.2023.02.056.

E, H-P, Kong, JAN, Chen, W-C, Chen, C-C, Cheng, C-H & Liu, C-Y 2022, 'Biocompatible spider silk-based metal-dielectric fiber optic sugar sensor', *Biomedical Optics Express*, vol. 13, no. 9, p. 4483. doi: 10.1364/boe.462573.

Erdogan, T 1997, 'Fiber grating spectra', *Journal of Lightwave Technology*, vol. 15, no. 8, pp. 1277–1294, <http://ieeexplore.ieee.org/document/618322/>.

Fu, C, Porter, D & Shao, Z 2009, 'Moisture Effects on Antheraea pernyi Silk's Mechanical Property', *Macromolecules*, vol. 42, no. 20, pp. 7877–7880. doi: 10.1021/MA901321K.

Gu, P, Tani, M, Hyodo, M, Sakai, K & Hidaka, T 1998, 'Generation of cw-Terahertz radiation using a two-longitudinal-mode laser diod', *Japanese Journal of Applied Physics, Part 2: Letters*, vol. 37(8 SUPPL. B), pp. 12291–12297. doi: 10.1143/jjap.37.l976.

Guo, B, Yao, Y, Yang, Y-F, Yuan, Y-J, Jin, L, Yan, B & Zhang, J-Y 2015, 'Dual-wavelength rectangular pulse erbium-doped fiber laser based on topological insulator saturable absorber. *Photonics Research*, vol 3, no. 3, p. 94. doi: 10.1364/prj.3.000094.

Han, Y-G, Tran, TVA, Kim, S-H & Lee, SB 2005, 'Development of a multiwavelength Raman fiber laser based on phase-shifted fiber Bragg gratings for long-distance remote-sensing applications', *Optics Letters*, vol. 30, no. 10, p. 1114. doi: 10.1364/ol.30.001114.

Hey Tow, K, Chow, DM, Vollrath, F, Dicaire, I, Gheysens, T & Thevenaz, L 2018, 'Exploring the Use of Native Spider Silk as an Optical Fiber for Chemical Sensing', *Journal of Lightwave Technology*, vol. 36, no. 4, pp. 1138–1144, viewed 28 August 2022, <http://ieeexplore.ieee.org.>

Huby, N *et al.* 2013a, 'Native spider silk as a biological optical fiber', *Applied Physics Letters*, vol. 102, no. 12, viewed 17 August 2023, </aip/apl/article/102/12/123702/25032/Native-spider-silk-as-a-biological-optical-fiber>.

Huby, N *et al.* 2013b, 'Native spider silk as a biological optical fiber', *Applied Physics Letters*, vol. 102, no. 12, p. 123702, viewed 28 August 2022, <https://aip.scitation.org/doi/abs/10.1063/1.4798552>.

Ibarra-Escamilla, B *et al.* 2018, 'Dissipative Soliton Resonance in a Thulium-Doped All-Fiber Laser Operating at Large Anomalous Dispersion Regime', *IEEE Photonics Journal*, vol. 10, no. 5, pp. 1–6. doi: 10.1109/JPHOT.2018.2870572.

Jasem, IN, Abdullah, HH & Jalal Abdulrazzaq, M 2023, 'Dual-Wavelength Passively Q-Switched Erbium-Doped Fiber Laser Incorporating Calcium Carbonate Nanoparticles as Saturable Absorber', *Journal of Nanotechnology* 2023. doi: 10.1155/2023/8858582.

Jiang, M, Lin, B, Shum, PP, Tjin, SC & Dong, X 2011, 'Frequency tunable microwave generation based on a dual-wavelength single-longitudinal-mode fiber laser incorporating a phase-shifted grating', *Optics InfoBase Conference Papers*, pp. 1142–1144.

Kashiwagi, K, Yamashita, S, Kashiwagi, K & Yamashita, S 2010, 'Optical Deposition of Carbon Nanotubes for Fiber-based Device Fabrication', *Frontiers in Guided Wave Optics and Optoelectronics*, viewed 30 October 2023, <https://www.intechopen.com/chapters/8444>.

Kiseleva, AP, Krivoshapkin, PV & Krivoshapkina, EF 2020, 'Recent Advances in Development of Functional Spider Silk-Based Hybrid Materials', *Frontiers in Chemistry*, vol. 8(June), pp. 1–20. doi: 10.3389/fchem.2020.00554.

Kleine-Ostmann, T & Nagatsuma, T 2011, 'A review on terahertz communications research', *Journal of Infrared, Millimeter, and Terahertz Waves*, vol. 32, no. 2, pp. 143–171. doi: 10.1007/s10762-010-9758-1.

Krzempek, K, Sobon, G & Abramski, KM 2013, 'DFG-based mid-IR generation using a compact dual-wavelength all-fiber amplifier for laser spectroscopy applications', *Optics Express*, vol. 21, no. 17, p. 20023. doi: 10.1364/oe.21.020023.

Li, G, He, J, Yan, B, Shi, B, Liu, J, Zhang, B & Yang, K 2019, 'Dual-wavelength passively Q-switched Er-doped fiber laser based on a MoSSe saturable absorber', *OSA Continuum*, vol. 2, no. 1, p. 192. doi: 10.1364/osac.2.000192.

Li, J *et al.* 2022, 'Spider Silk-Inspired Artificial Fibers', *Advanced Science*, vol. 9, no. 5, p. 2103965, viewed 28 September 2022, <https://onlinelibrary.wiley.com/doi/10.1002/advs.202103965>.

Lin, CY, Chern, GW & Wang, LA 2001, 'Periodical corrugated structure for forming sampled fiber Bragg grating and long-period fiber grating with tunable coupling strength', *Journal of Lightwave Technology*, vol. 19, no. 8, pp. 1212–1221. doi: 10.1109/50.939803.

Liu, L *et al.* 2013, 'Dual-wavelength passively Q-switched Erbium doped fiber laser based on an SWNT saturable absorber', *Optics Communications*, vol. 294, pp. 267–270. doi: 10.1016/j.optcom.2012.11.094.

Muhammad, NAM, Awang, NA & Basri, H 2023, 'Recent advancements review in zinc oxide and titanium dioxide saturable absorber for ultrafast pulsed fiber laser', *Optik*, vol. 283(September 2022), p. 170855. doi: 10.1016/j.ijleo.2023.170855.

Muhammad, NAM, Awang, NA, Basri, H, Latif, AA, Zalkepali, NUHH, Zamri, AZM & Mahmud, NNHEN 2024, 'Steady Q-switched erbium-doped fiber laser pulse generation by exploiting spider silk as a passive saturable absorber', *Optics and Laser Technology*, vol. 169(September 2023), p. 110170. doi: 10.1016/j.optlastec.2023.110170.

Muhammad, NAM, Awang, NA, Zalkepali, NUHH, Mahmud, NNHEN & Basri, H 2022, 'Q-switched fiber laser using a polysulfone membrane enhanced with biosynthesized zinc oxide and titanium dioxide nanoparticles for use as saturable absorber', *Laser Physics*, vol. 32, no. 6, p. 065101, viewed at <https://iopscience.iop.org/article/10.1088/1555-6611/ac687d>.

Najm, MM, Nizamani, B, Al-Azzawi, AA, Hmood, JK, Abdullah, MN & Harun, SW 2023, 'Generation of dual-wavelength Q-switched laser pulses by employing Mo2Ti2AlC3 MAX phase film', *Optical Fiber Technology*, vol. 81(August), p. 103566. doi: 10.1016/j.yofte.2023.103566.

Pan, S & Yao, J 2009a, 'A wavelength-switchable single-longitudinal-mode dual-wavelength erbium-doped fiber laser for switchable microwave generation', *Optics Express*, vol. 17, no. 7, p. 5414. doi: 10.1364/oe.17.005414.

Pan, S & Yao, J 2009b, 'Frequency-switchable microwave generation based on a dual-wavelength single-longitudinal-mode fiber laser incorporating a high-finesse ring filter', *Optics Express*, vol. 17, no. 14, p. 12167. doi: 10.1364/oe.17.012167.

Qiao, X *et al.* 2017, 'Synthetic Engineering of Spider Silk Fiber as Implantable Optical Waveguides for Low-Loss Light Guiding', *ACS Applied Materials & Interfaces*, vol. 9, no. 17,

pp. 14665–14676, viewed 28 August 2022, <https://pubs.acs.org/doi/pdf/10.1021/acsami.7b01752>.

Sardar, MR, Faisal, M & Ahmed, K 2021, 'Simple hollow core photonic crystal fiber for monitoring carbon dioxide gas with very high accuracy', *Sensing and Bio-Sensing Research*, vol. 31, p. 100401. doi: 10.1016/j.sbsr.2021.100401.

Sharma, U, Kim, CS, Kang, JU & Fried, NM 2004, 'Highly stable tunable dual-wavelength Q-switched fiber laser for DIAL applications', *Optics InfoBase Conference Papers*, vol. 16, no. 5, pp. 1277–1279.

Soltanian, MRK, Ahmad, H, Alavi, SE & Amiri, IS 2015, 'Dual-Wavelength Erbium-Doped Fiber Laser to Generate Terahertz Radiation Using Photonic Crystal Fiber', *Journal of Lightwave Technology*, vol. 33, no. 24, pp. 5038-5046, viewed 27 December 2023, <https://opg.optica.org/abstract.cfm?uri=jlt-33-24-5038>.

Tang, M, Minamide, H, Wang, Y, Notake, T, Ohno, S & Ito, H 2011, 'Tunable terahertz-wave generation from DAST crystal pumped by a monolithic dual-wavelength fiber laser', *Optics Express*, vol. 19, no. 2, p. 779. doi: 10.1364/oe.19.000779.

Vehoff, T, Glišović, A, Schollmeyer, H, Zippelius, A & Salditt, T 2007, 'Mechanical properties of spider dragline silk: Humidity, hysteresis, and relaxation', *Biophysical Journal*, vol. 93, no. 12, pp. 4425–4432. doi: 10.1529/biophysj.106.099309.

Wang, M, Chen, C, Li, Q, Huang, K & Chen, H 2015, 'Photonic generation of tunable microwave signal using a passively Q-switched dual-wavelength fiber laser', *Microwave and Optical Technology Letters*, vol. 57, no. 1, pp. 166–168, viewed at <http://onlinelibrary.wiley.com/doi/10.1002/mop.21988/abstract>.

Yao, Y, Chen, X, Dai, Y & Xie, S 2006, 'Dual-wavelength erbium-doped fiber laser with a simple linear cavity and its application in microwave generation', *IEEE Photonics Technology Letters*, vol. 18, no. 1, pp. 187–189. doi: 10.1109/LPT.2005.861309.

Yin, B, Wu, S, Wang, M, Li, H, Wang, Q, Wu, B & Liu, W 2019, 'High-sensitivity refractive index and temperature sensor based on cascaded dual-wavelength fiber laser and SNHNS interferometer', *Optics* Express, vol. 27, no. 1, pp. 252–264, viewed 27 December 2023 at <https://opg.optica.org/viewmedia.cfm?uri=oe-27-1-252&seq=0&html=true>.

Yu, J, Jia, Z, Xu, L, Chen, L, Wang, T & Chang, GK 2006, 'DWDM optical millimeter-wave generation for radio-over-fiber using an optical phase modulator and an optical interleaver', *IEEE Photonics Technology Letters*, vol. 18, no. 13, pp. 1418–1420. doi: 10.1109/LPT.2006.877226.

Yusoff, RAM, Kasim, N, Jafry, AAA, Munajat, Y, Harun, SW & Suliman, MI 2019, 'Q-Switched dual-wavelength erbium-doped fiber laser using graphene as a saturable absorber', *Journal of Physics: Conference Series*, vol. 1371, no. 1. doi: 10.1088/1742-6596/1371/1/012007.

Zalkepali, NUHH, Awang, NA, Latif, AA, Zakaria, Z, Yuzaile, YR & Mahmud, NNHEN 2020, 'Switchable dual-wavelength Q-switched fiber laser based on sputtered indium tin oxide as saturable absorber', *Results in Physics*, vol. 17, p. 103187. doi: 10.1016/j.rinp.2020.103187.

Zhang, C, Sun, J, Zheng, S & Jian, S 2012, 'A simple mechanism to suppress the mode competition for stable and tunable dual-wavelength erbium-doped fiber lasers', *Advanced Materials Research*, vol. 571, pp. 496–499. doi: 10.4028/www.scientific.net/AMR.571.496.